Stability Analysis of Traveling Wave Solution for Gravity-Driven Flow

A. G. Egorov[a] , R. Z. Dautov [a], J. L. Nieber [b] and A. Y. Sheshukov [b] *

[a]Kazan State University, Kremlyovskaya 18, Kazan, 420008, Russia

[b]University of Minnesota, 1390 Eckles Avenue, Saint Paul, MN 55108, U.S.A.

A linear stability analysis was performed for three models of flow in unsaturated porous media to determine the conditions for growth of small perturbations. The models considered include the conventional Richards equation (RE), a sharp front Richards equation (SFRE) and an extended Richards equation (RRE). The first two models are based on the use of an equilibrium capillary pressure-saturation function, while the third model is derived using a dynamic capillary pressure-saturation function represented by a relaxation coefficient. A traveling wave solution was formulated for each of the governing equations and used as the basic solution of each model. The stability analysis was based on imposing a small perturbation to the basic solution. The RE model yields only the well-known monotonically decreasing saturation profile toward the wetting front, and the wetting front is unconditionally stable. The SFRE model by its nature has a monotonically increasing saturation profile toward the front and an abrupt drop to the initial saturation. This flow is unconditionally unstable. The RRE model is distinct from the others in that it is the only model that is able to produce truly non-monotonic saturation profiles. The wetting front for the RRE model is conditionally stable, *i.e.* stable for high frequency perturbations, and unstable otherwise. This leads to the existence of a wave-number for maximum amplification, which should relate to the dimensions of fingers in unstable flow.

1. Introduction

The phenomenon of gravity-driven unstable flow has attracted much interest during the last three decades. Many mathematical models have been developed to attempt to model this phenomenon [1, 2, 3, 4]. To describe the fingering, the mathematical model to be developed must bear at least two principal features: (i) the model must be able to generate initial unstable growth of small perturbations, and (ii) it must be able to promote persistence of the initially growing perturbations by limiting lateral spreading behind the unstable front. The experimental results presented by Glass et al. [3] and the physically based theory described by Glass et al. [3] and Nieber [4] demonstrate that the second

*The authors wish to acknowledge support under NATO Collaborative Linkage Grant 978242. Partial support was also provided by the Army High Performance Computing Research Center under the auspices of the Department of the Army, Army Research Laboratory cooperative agreement number DAAD19-01-2-0014, the content of which does not necessarily reflect the position or the policy of the government, and no official endorsement should be inferred.

of these features, finger persistence, is dominated by hysteresis in the capillary pressure-saturation relation. This issue seems to be well understood and designates hysteresis as a necessary mechanism that must be incorporated in a model of gravity-driven unstable flow.

Finger generation and associated aspects of wetting front instability have been broadly discussed in the literature [1, 2, 5, 6, 7]. Nonetheless, appropriate mechanisms causing finger generation and models capable of describing it have yet to be discovered. In this paper we study the wetting front instability analyzing three distinct models presented to date:
(i) the conventional Richards equation (RE),
(ii) a sharp front Richards equation (SFRE) [8], and
(iii) an extended Richards equation with a non-equilibrium (relaxation) pressure-saturation function (RRE) [9].
In sections 2 through 4 we consider a traveling wave solution for the three models and apply a linear stability analysis to each of those solutions. Results of the stability analysis are presented in sections 2 to 4, and then discussed in section 5.

2. Richards' equation (RE)

2.1. Basic solution

The conventional Richards equation for the flow of water in unsaturated porous media may be written in dimensionless form as

$$\frac{\partial s}{\partial t} - \nabla \cdot K(s)\nabla p + \frac{\partial}{\partial z} K(s) = 0 \tag{1}$$

$$p = P(s) \tag{2}$$

where s is the effective saturation ($0 \leq s \leq 1$), p is the water pressure, K is the relative hydraulic conductivity being a convex and monotonically increasing function of s, P is the equilibrium pressure being a monotonically increasing function of s, and z is the vertical coordinate taken positive downward. Pressure and spatial coordinates are normalized on air-entry pressure.

The traveling wave solution for (1) and (2) with the traveling wave coordinate ξ

$$s = s(\xi), \quad \xi = z - vt \tag{3}$$

was developed by Philip [10]. The boundary conditions

$$s(-\infty) = s_-, \quad s(+\infty) = s_+, \quad s_- > s_+ \tag{4}$$

specify values of the saturation ahead (s_+) of the wetting front (in the 'dry' region) and behind (s_-) the wetting front (in the 'wet' region), while the velocity of the wetting front v may be defined as

$$v = \frac{K(s_+) - K(s_-)}{s_+ - s_-} \tag{5}$$

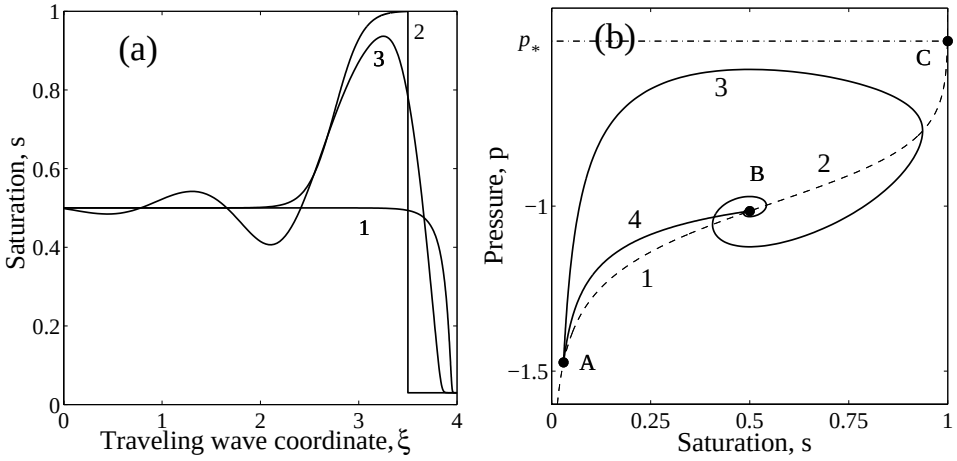

Figure 1. (a) Water saturation profiles for three distinct models: 1 – the RE model; 2 – the SFRE model; 3 – the RRE model (non-monotonic profile), and (b) their trajectories in the phase plane. Point A (s_+, p_+) corresponds to the initial state, while point B (s_-, p_-) corresponds to the final state. The equilibrium line $p = P(s)$ is shown by the dashed line. The trajectory 1 for the RE model follows the equilibrium curve. For the SFRE model, there is an abrupt jump in pressure and saturation from point A to point C and then gradual reduction in saturation to point B via the equilibrium curve. Trajectories 3 and 4 correspond respectively to the non-monotonic and monotonic regimes of the RRE model.

Substituting (3) and (5) into (1) and (2), and integrating the resulting ordinary differential equation with (4), the solution of the problem is obtained as

$$\xi - \xi_* = \int_s^{s_*} \frac{D(s)\,ds}{v(s - s_+) - K(s) + K(s_+)} \tag{6}$$

where $D(s) = KP'$ is the diffusivity, and s_* $(s_+ < s_* < s_-)$ is the saturation at the arbitrary point ξ_*. Arbitrariness of s_* indicates that the Philip's solution (6) is valid with any spatial shift. We also emphasize that the denominator in (6) is negative for $s \in (s_+, s_-)$ and equal to zero at both ends $s = s_+$ and $s = s_-$, because $K(s)$ is considered to be a convex function. As a result, $s(\xi)$ monotonically decreases from s_- at $\xi = -\infty$ to s_+ at $\xi = +\infty$ (curve 1 in Figure 1a).

2.2. Stability analysis

A standard linear perturbation technique is applied to study the stability of the traveling wave solution. Let ε be a small parameter. The perturbed saturation field is

$$s = s_0(\xi) + \varepsilon e^{i(\omega_1 x + \omega_2 y)} e^{kt} s_1(\xi) + O(\varepsilon^2) \tag{7}$$

where s_0 is the basic solution (6), s_1 is an unknown function which allows for a spatial variation in the z direction, ω_1 and ω_2 are the characteristic wave numbers in the x and y directions respectively, and k is the amplification or growth factor. According to (7) a perturbation will grow in magnitude if $k > 0$, and diminishes if $k < 0$.

Substituting (7) into (1) and (2), and introducing new variables $S = s_1/s_0'$ and $\sigma = s_0(\xi)$ instead of s_1 and ξ respectively, the resulting perturbation equation to the first order in ε is obtained for $S(\sigma)$

$$\omega^2 D(\sigma)S - \frac{d}{d\sigma}\left(R(\sigma)\frac{dS}{d\sigma}\right) = -kS \tag{8}$$

where $\omega^2 = \omega_1^2 + \omega_2^2$, and $R(\sigma) = \left(K(\sigma) - K(s_+) + v(s_+ - \sigma)\right)^2 / D(\sigma)$. Equation (8) is defined within the finite interval $s_+ < \sigma < s_-$ and subject to the following boundary conditions

$$\lim_{\sigma \to s_-} R(\sigma)\frac{dS}{d\sigma} = 0, \qquad \lim_{\sigma \to s_+} R(\sigma)\frac{dS}{d\sigma} = 0 \tag{9}$$

The stability analysis of the basic solution is now reduced to finding the eigenvalues of $k(\omega)$ for the problem (8),(9). Without proof, the following theorem is stated.

Theorem 1 *For any $\omega > 0$ there exists a maximum eigenvalue $k_0(\omega)$ for (8), (9); k_0 monotonically decreases with ω and $k_0(0) = 0$, $k_0(\infty) = -\infty$.*

This theorem dictates that a traveling wave solution for the Richards model is stable for any perturbation mode. This result was found earlier by Diment and Watson [5] based on numerical analysis of a perturbation equation similar to (8).

3. Sharp front Richards equation (SFRE)

3.1. Basic solution

Experimental evidence [3, 8] shows that a sharp wetting front is observed for wetting of initially dry porous media with $s_+ \ll 1$. The saturation on the advancing front has a jump from s_+ to some value s_*. According to Glass et al. [3], the corresponding value $p_* = P(s_*)$ on the wetting side of the front is close to the water entry value of the water pressure. This assumption modifies the RE model to the SFRE model for the wetting front advancement introduced in [8]. The SFRE model is based on the assumption that the porous medium is divided by the wetting front $z = z_*(t)$ into two regions: the porous medium remains initially dry with $s = s_*$ for $z > z_*$, and the Richards equation (1),(2) is valid for $z < z_*$. The model by Selker et al. [8] is of this type. Saturation at the wetting side of the front is given by

$$z = z_* - 0: \quad s = s_* \tag{10}$$

An additional condition on the advancing front is mass conservation:

$$z = z_*: \quad (s_* - s_+)\frac{dz_*}{dt} = K(s_*) - K(s_+) - K(s_*)\frac{\partial p}{\partial z}(s_*) \tag{11}$$

The traveling wave solution for the problem (1),(2),(10), and (11) is derived by Selker et al. [8]. For the wetted region $\xi < \xi_*$ ($\xi_* = z_* - vt$), the solution has the same form as the Philip's solution (5), and (6). However, the saturation profile for the SFRE model monotonically increases from s_- at $\xi = -\infty$ to s_* at $\xi = \xi_*$ with ξ, and then abruptly drops to the initial dry value s_+ (curve 2 in Figure 1a).

3.2. Stability analysis

The preceding linear perturbation technique with variables S and σ defined in the previous section is applied, and the perturbation equation is given by (8). Now, equation (8) is valid within the interval $\sigma \in (s_-, s_*)$ and subject to the following boundary conditions:

$$\lim_{\sigma \to s_-} R(\sigma)\frac{dS}{d\sigma} = 0, \qquad R(\sigma)\frac{dS}{d\sigma} = k\sigma S \quad \text{for} \quad \sigma = s_* \tag{12}$$

Again without proof we state the theorem.

Theorem 2 *For any $\omega > 0$ there exists a maximum eigenvalue $k_0(\omega)$ for (8) and (12); k_0 monotonically increases with ω and $k_0(0) = 0$, $k_0(\infty) = \infty$.*

Theorem 2 dictates that the traveling wave solution for the SFRE model is unstable for any perturbation mode.

4. Relaxation model (RRE)

4.1. Basic solution

The extension of the Richards equation to take into account dynamic memory effects was suggested by Hassanizadeh and Gray [11, 9]. The key point in the theory of dynamic memory effects is the rejection of the equilibrium relationship (2) between saturation s and pressure p and replacing it with a kinetic equation such as

$$\tau\frac{\partial s}{\partial t} = p - P(s) \tag{13}$$

where the dimensionless relaxation coefficient τ being positive is considered to be a function of the material properties of the medium and depends only on the saturation. Substituting the variables (3) into the system of equations (1) and (13) and integrating the mass balance equation results in the following dynamic system

$$\begin{aligned} -K(s)\frac{dp}{d\xi} &= v(s - s_+) + K(s_+) - K(s) \\ -\tau v\frac{ds}{d\xi} &= p - P(s) \end{aligned}$$

where the wetting front velocity v is defined by (5).

We consider the phase (s, p) portrait of the dynamic system. The phase portrait is specified by two singular points: (s_+, p_+) and (s_-, p_-). Both points belong to the equilibrium curve $p_+ = P(s_+)$ and $p_- = P(s_-)$. The trajectory of the traveling wave begins at the saddle type singular point (s_+, p_+) and ends at the second one (s_-, p_-). The type of the second singular point characterizes the traveling wave type. There are two modes. Point (s_-, p_-) represents either a nodal type for the case of $\tau(s_-) < \tau_F(v, s_-)$, or focus type otherwise, where the critical value of the relaxation coefficient separating these types is defined as

$$\tau_F = \frac{\left(P'(s_-)\right)^2 K(s_-)}{4v\left(K'(s_-) - v\right)}$$

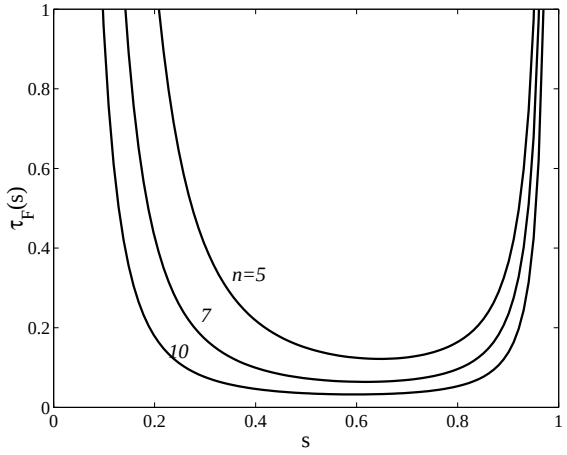

Figure 2. Critical value of the relaxation coefficient as a function of s for different n.

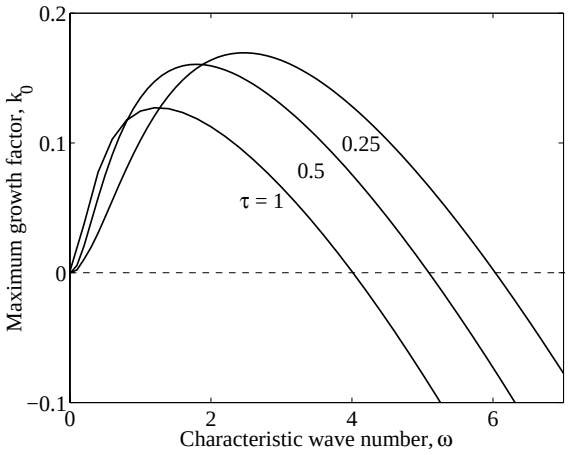

Figure 3. Growth factor vs. characteristic wave number for the RRE model for three values of constant relaxation coefficient τ.

where the prime indicates the derivative with respect to s. In the case of the focus type singular point, integral curves spiral to the singular point (curve 3 in Figure 1b), and it leads to a non-monotonic profile of $s(\xi)$ (curve 3 in Figure 1a). For a nodal type singular point the integral curve (curve 4 in Figure 1b) behaves similarly to that for the RE model, and the profile of $s(\xi)$ lies very close to that by Philip's solution (curve 1 in Figure 1a).

The traveling wave solution for the RRE model, being monotonic for the low values of τ, becomes non-monotonic for the higher values of τ. It is interesting to determine which type of soil the second mode may occur. Hassanizadeh [12] estimates that for sandy soils the dimensionless relaxation time likely ranges from 1 to 2000. To evaluate τ_F we assume $s_- \gg s_+$. For this case, $v = K(s_-)/s_-$, and τ_F is a function only of s_-:

$$\tau_F = \tau_F(s_-) = \frac{(s_- P'(s_-))^2}{4\,(s_- K'(s_-) - K(s_-))}$$

This function is presented in Figure 2 for a Van Genuchten-Mualem model:

$$P(s) = -\left(s^{-1/m} - 1\right)^{1/n}, \quad K(s) = s^{1/2}\left(1 - \left(1 - s^{1/m}\right)^m\right)^2, \quad m = 1 - 1/n$$

for different values of n. It is seen that within the range $0.2 < s_- < 0.9$ the critical relaxation time τ_F does not exceed unity. Comparing this value to the data by Hassanizadeh [12], one may say that non-monotonic behavior of the process definitely occurs in sandy soils. Whether it will occur for finer textured soils will be assessed when relaxation data for finer textured soils become available.

4.2. Stability analysis

The linear stability analysis used previously is now focused on finding the eigenvalue k_0 with maximum real part for the perturbation equation. In contrast to the preceding

stability analysis, the perturbation equation turns out to not be self-adjoint and makes the theoretical analysis complicated. Therefore, we study this problem numerically. We use a finite-difference approximation of the perturbation equation on fine non-uniform grids. The resulting algebraic eigenvalue problem is solved by standard methods of linear algebra. The obtained results were validated by (i) refining the grid, (ii) applying different approximation methods, and (iii) using different iterative procedures to solve the grid equations.

The eigenvalue k_0 turned out to be real in all simulations. Figure 3 shows k_0 as a function of ω for the Van Genuchten-Mualem model with $n = 10$, $s_+ = 0.03$, $s_- = 0.5$, and different constant values of τ. We also performed simulations for various functions $\tau(s)$. From the physical standpoint, one may reason that $\tau(s)$ grows to infinity as s approaches zero. Therefore, in calculations we use several different functions: $\tau(s) = \tau_0 s^{-\beta}$, where $\beta = 0.5$ and 1, and $\tau(s) = P'(s)$. The latter choice also gives unlimited growth of τ as s approaches unity. The function $k_0(\omega)$ was found to be qualitatively the same as those shown in Figure 3 for all of the calculations.

5. Discussion

In this paper we analyzed three models: the RE model, the SFRE model and the RRE model, to study gravity-driven unstable flow. The analysis concludes that fingering in unsaturated porous media can not be described by either the RE model, or the SFRE model. The RE model turned out to be unconditionally stable, and small perturbations of the basic solution *always* damp out. The SFRE model turned out to be unconditionally unstable, and *any* small perturbations must grow with time. The higher the frequency, the faster the rate of growth of perturbations. The instability produced by the SFRE model is similar to the persistence-free Saffman-Taylor instability [13]. It is known that unconditional instability produces a tree-like fractal structure because no fastest growing perturbation exists. However, experimentally observed fingers [3, 8] have a well-defined width that may be produced by another type of instability. The analysis provided in section 4 justifies that the RRE model leads to that type of instability. Calculations performed for the RRE model demonstrate that there exists a maximum point $(\omega_{\max}, k_{0\max})$ on the k_0 vs. ω curves shown in Figure 3. This means that perturbations with wavelength $L_{\max} = 2\pi/\omega_{\max}$ grow faster than perturbations with other wavelengths.

The parameters $L_{\max}$ and $k_{\max}$ as functions of relaxation coefficient τ are illustrated in Figure 4 for $n = 10$, $s_+ = 0.03$ and $s_- = 0.5$. Figure 4a shows that $k_{0\max}$ becomes negative and, as a result, the process is stable for small values of τ. The critical value of τ when $k_{0\max}$ changes sign corresponds to the parameter τ_F introduced in section 4. Therefore, instability of the gravity-driven flow seems to be associated with a non-monotonicity of the moisture content profile $s(\xi)$. Monotonic profiles obtained by the RRE model for a small values of τ are stable, the same as the ones obtained by the RE model. Non-monotonic profiles obtained by the RRE model for large values of τ are unstable, the same as the ones obtained by the SFRE model. The difference in instability behavior for the RRE and the SFRE models seems to be caused by different advancing front width of the traveling wave solution. The advancing front has infinitesimal width for the SFRE model, while the relaxation mechanism diffuses the front to a finite width for the RRE model.

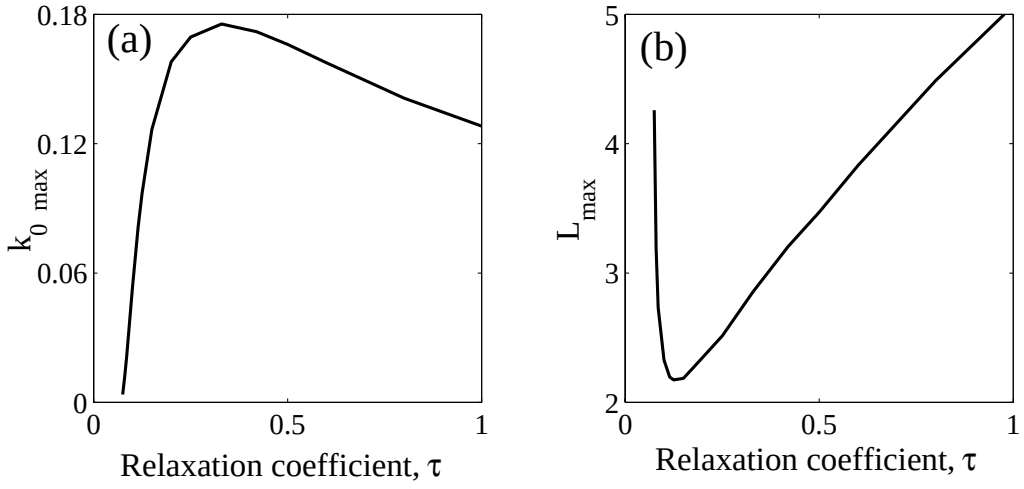

Figure 4. (a) Maximum growth factor, $k_{0\,\max}$, and (b) maximum perturbation wavelength, $L_{\max}$, vs. relaxation coefficient τ.

The parameter $L_{\max}$ may be used as a measure of the width between the center points of adjacent fingers. From Figure 4b it is seen that for the relaxation parameter in the reasonable range of 0.25 to 1.0, the value of $L_{\max}$ ranges from about 2.5 to 5. Since $L_{\max}$ is scaled to the air-entry pressure of the porous medium this means that the distance between finger centers should be on the order of 2.5 to 5 times the air-entry pressure of the porous medium.

In this work we neglected hysteretic effects in studying the fingering phenomenon. Our analysis focused on the short time period immediately after introducing a perturbation but does not apply for a long time. It is obvious that hysteresis must be incorporated in the model to study finger growth and its persistence. This issue will be discussed in another paper.

REFERENCES

1. P. A. C. Raats, Soil Sci. Soc. Am. Proc. 37 (1973) 681.
2. J. R. Philip, Soil Sci. Soc. Am. Proc. 39 (1975) 1042.
3. R. J. Glass, T. S. Steenhuis and J.-Y. Parlange, Soil Sci. 148 (1989) 60.
4. J. L. Nieber, Geoderma 70 (1996) 207.
5. G. A. Diment and K. K. Watson, Water Resour. Res. 19 (1983) 1002.
6. V. Kapoor, Transp. Porous Media 25 (1996) 313.
7. X. Du, T. Yao, W. D. Stone and J. M. H. Hendrickx, Water Resour. Res. 37 (2001) 1869.
8. J. S. Selker, J.-Y. Parlange and T. Steenhuis, Water Resour. Res. 28 (1992) 2523.
9. S. M. Hassanizadeh and W. G. Gray, Water Resour. Res. 29 (1993) 3389.
10. J. R. Philip, Soil Sci. 84 (1957) 257.
11. S. M. Hassanizadeh and W. G. Gray, Adv. Water Resour. 13 (1990) 169.

12. S. M. Hassanizadeh, Proc. 4th Int. Conf. on Civil. Eng. (Teheran, Iran) 4 (1997) 141.
13. P. G. Saffman and G. Taylor, Proc. Royal Soc. London, Ser. A 245 (1958) 312.